

# A GENERAL LOW FREQUENCY ACOUSTIC RADIATION CAPABILITY FOR NASTRAN

by

G.C. Everstine, F.M. Henderson, E.A. Schroeder, and R.R. Lipman

Numerical Mechanics Division  
David W. Taylor Naval Ship Research and Development Center  
Bethesda, Maryland 20084-5000

## ABSTRACT

A new capability called NASHUA is described for calculating the radiated acoustic sound pressure field exterior to a harmonically-excited arbitrary submerged 3-D elastic structure. The surface fluid pressures and velocities are first calculated by coupling a NASTRAN finite element model of the structure with a discretized form of the Helmholtz surface integral equation for the exterior fluid. After the fluid impedance is calculated, most of the required matrix operations are performed using the general matrix manipulation package (DMAP) available in NASTRAN. Far-field radiated pressures are then calculated from the surface solution using the Helmholtz exterior integral equation. Other output quantities include the maximum sound pressure levels in each of the three coordinate planes, the rms and average surface pressures and normal velocities, the total radiated power, and the radiation efficiency. The overall approach is illustrated and validated using known analytic solutions for submerged spherical shells subjected to both uniform and non-uniform applied loads.

## INTRODUCTION

A fundamental problem of interest in acoustics is the calculation of the far-field acoustic pressure field radiated by a general submerged three-dimensional elastic structure subjected to internal time-harmonic loads. This problem is usually solved by combining a finite element model of the structure with a fluid loading computed using either finite element [1-3] or boundary integral equation [4-10] techniques.

Although both approaches are computationally expensive for large structural models, the fluid finite element approach is burdened with the additional complications caused by the approximate radiation boundary condition at the outer fluid boundary, the requirements on mesh size and extent, and the difficulty of generating the fluid mesh [1,3].

In contrast, the boundary integral equation (BIE) approach for generating the fluid loading is mathematically exact (except for surface discretization error) and requires no additional modeling effort to convert an existing model of a dry structure for use in submerged analyses. The savings in engineering time, however, is partially offset by the somewhat greater computing costs associated with the BIE approach.

Although several general BIE acoustic radiation capabilities have been developed previously, none was developed for the widely-used, nonproprietary structural analysis code NASTRAN. Here we present a new capability known as

NASHUA which couples a NASTRAN finite element model of a dry structure with a fluid loading calculated by a discretized form of the Helmholtz surface integral equation.

The primary purposes of this paper are to describe in detail the theoretical basis for NASHUA and to demonstrate its validity by showing results of radiation calculations for the elementary problems of uniformly-driven and sector-driven spherical shells. Detailed user's information will not be presented here since a user's guide for NASHUA was published previously [11].

## THEORETICAL APPROACH

We wish to calculate the far-field acoustic pressure field radiated by a general submerged three-dimensional elastic structure subjected to internal time-harmonic loads. In general, our approach combines in a highly automated fashion a finite element model of the structure with a Helmholtz boundary integral equation model of the fluid.

### The Structure

The dry structure, when modeled with finite elements in a conventional way, results in the equation of motion in the frequency domain

$$(-\omega^2 M + i\omega B + K)u = F \quad (1)$$

where  $M$ ,  $B$ , and  $K$  are the structural mass, viscous damping, and stiffness matrices, respectively,  $\omega$  is the circular frequency of excitation,  $F$  is the complex amplitude of the applied force, and  $u$  is the complex amplitude of the displacement vector. The time dependence  $\exp(i\omega t)$  has been suppressed. For structures with material damping or a nonzero loss factor,  $K$  is complex. We note from Equation (1) that the structural impedance matrix (the ratio of force to velocity) is

$$Z_s = i\omega M + B - iK/\omega \quad (2)$$

### The Exterior Fluid

For the fluid, the pressure  $p$  satisfies the reduced wave equation

$$\nabla^2 p + k^2 p = 0 \quad (3)$$

where  $k = \omega/c$  is the acoustic wave number, and  $c$  is the speed of sound in the fluid. Equivalently,  $p$  is the solution of the Helmholtz integral equation [12]

$$\int_S p(\underline{x})(\partial D(\underline{r})/\partial n)dS - \int_S q(\underline{x})D(\underline{r})dS = \begin{cases} p(\underline{x}')/2, & \underline{x}' \text{ on } S \\ p(\underline{x}'), & \underline{x}' \text{ in } E \end{cases} \quad (4)$$

where  $S$  and  $E$  denote surface and exterior fluid points, respectively,  $r$  is the distance from  $\underline{x}$  to  $\underline{x}'$  (Figure 1),  $D$  is the Green's function

$$D(\underline{r}) = e^{-ikr}/4\pi r \quad (5)$$

and

$$q = \partial p / \partial n = -i\omega\rho v \quad (6)$$

where  $\rho$  is the density of the fluid, and  $v$  is the outward normal component of velocity on  $S$ . As shown in Figure 1,  $\underline{x}$  in Equation (4) is the position vector for a typical point  $P_j$  on the surface  $S$ ,  $\underline{x}'$  is the position vector for the point  $P_i$  which may be either on the surface or in the exterior field  $E$ , the vector  $\underline{r} = \underline{x}' - \underline{x}$ , and  $\underline{n}$  is the unit outward normal at  $P_j$ . We denote the lengths of the vectors  $\underline{x}$ ,  $\underline{x}'$ , and  $\underline{r}$  by  $x$ ,  $x'$ , and  $r$ , respectively. The normal derivative of the Green's function  $D$  appearing in Equation (4) can be evaluated as

$$\partial D(\underline{r}) / \partial n = (e^{-ikr}/4\pi r) (ik + 1/r) \cos \beta \quad (7)$$

where  $\beta$  is defined in Figure 1.

The substitution of Equations (6) and (7) into the surface equation (4) yields

$$\begin{aligned} p(\underline{x}')/2 - \int_S p(\underline{x}) (e^{-ikr}/4\pi r) (ik + 1/r) \cos \beta \, dS \\ = i\omega\rho \int_S v(\underline{x}) (e^{-ikr}/4\pi r) dS \end{aligned} \quad (8)$$

where  $\underline{x}'$  is on  $S$ . This equation can be interpreted as an integral equation relating the pressure  $p$  and normal velocity  $v$  on  $S$ . If Equation (8) is discretized for numerical computation, we obtain the matrix equation

$$E p = C v \quad (9)$$

on  $S$ . With low-order approximations to the integrals,  $E$  can be evaluated simply as

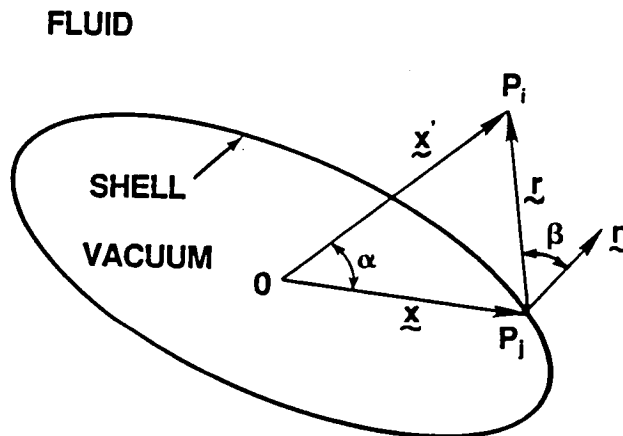


Figure 1 - Notation for Helmholtz Integral Equations

$$E_{ij} = -(e^{-ikr}/4\pi r) (ik + 1/r) (\cos \beta_{ij}) A_j, \quad i \neq j \quad (10)$$

where  $A_j$  is the area assigned to the point  $\underline{x}_j$ , and  $r = r_{ij} = |\underline{x}_i - \underline{x}_j|$ . Similarly,

$$C_{ij} = (i\omega \rho e^{-ikr}/4\pi r) A_j, \quad i \neq j \quad (11)$$

In general, surface areas in NASHUA are obtained from the NASTRAN calculation of the load vector resulting from an outwardly directed static unit pressure load on the structure's wet surface.

The use of low-order integration in Equations (10) and (11) yields roughly the same accuracy as would be obtained if linear shape functions were used for the variation of  $p$  and  $v$  over the element [7]. (This property is analogous to the situation in one-dimensional Newton-Cotes integration in which odd-point formulas are preferred to the next higher-order even-point formulas, since both have the same order of accuracy [13].) Moreover, the integration scheme selected is particularly easy to implement since it requires a knowledge only of the area assigned to each point rather than any information about the elements on the wet surface.

The above two formulas for  $E_{ij}$  and  $C_{ij}$  are applicable only for the off-diagonal terms ( $i \neq j$ ), because  $r$  vanishes for  $i = j$ . For this singular case, the integrals in Equation (8), which are in fact well-defined, must be evaluated by a different approach. Consider first the velocity integral in Equation (8). Following Chertock [14], if we assume that  $v$  is constant over a small circular patch of radius  $b_i$  centered at  $\underline{x}_i$ , then, from Equation (8),

$$C_{ii} = i\omega \rho \int_0^{2\pi} \int_0^{b_i} (e^{-ikr}/4\pi r) r dr d\theta \quad (12)$$

where  $b_i$  is selected so that  $\pi b_i^2 = A_i$ , the total area assigned to the point. The evaluation of this integral yields

$$C_{ii} = i\omega \rho A_i / 2\pi b_i \quad (13)$$

where

$$b_i = (A_i/\pi)^{1/2} \quad (14)$$

The evaluation of the "self term"  $E_{ii}$  is similar except that the curvature of the radiating surface must be taken into account because the singularity in the pressure term of Equation (8) is one order higher than that of the velocity term. Here we assume that  $p$  is constant over a small spherical cap located at  $\underline{x}_i$  and having curvature  $c_i$  and area  $A_i$ . Then, from Equation (1),

$$E_{ii} = 1/2 - \int_0^{2\pi} \int_0^{b_i} (e^{-ikr}/4\pi r) (ik + 1/r) (-rc_i/2) r dr d\theta \quad (15)$$

where we have used the approximation

$$\cos \beta = -rc_i/2 \quad (16)$$

The evaluation of this integral yields

$$E_{ii} = 1/2 + (1 + ikb_i) (c_i A_i)/(4\pi b_i) \quad (17)$$

where we interpret  $c_i$  as the mean curvature at  $x_i$ .

The use of  $b_i$  in Equation (13) and (17) facilitates the calculation of the self terms at points lying in planes of symmetry, since  $A_i$  is halved or quartered at such points, but  $b_i$  is computed from Equation (14) as if the full area at the point were applicable.

The need to know the mean curvatures at each wet point is the major impediment to full generality for the NASHUA procedure, since there is no mechanism built into NASTRAN that enables the user to extract the curvature of a surface at a point. NASHUA handles this problem by placing some minor restrictions on the analyst so that the curvatures can be computed for the commonly-occurring geometries of spheres, cylinders, conical sections, and flat sections. For other shapes, the user must insert a few lines of code into the NASHUA processor SURF to compute the curvature at each point, given its location.

In contrast to the situation for curvatures, the NASHUA requirement for surface areas and normals is handled with full generality, since the user defines the wet surface by applying a static, outwardly-directed, unit pressure load to that surface.

We note from Equation (9) that, if  $E^{-1}$  exists, the impedance matrix  $Z_f$  for the exterior fluid is

$$Z_f = A E^{-1} C \quad (18)$$

where  $A$  is the diagonal area matrix for the wet surface.

### The Coupled System

The structural and fluid impedance matrices given by Equations (2) and (18) cannot be added to yield the impedance matrix for the submerged structure since  $Z_s$  and  $Z_f$  are not conformable. The matrix  $Z_s$  has dimension  $s \times s$ , and  $Z_f$  has dimension  $f \times f$ , where  $s$  is the number of structural degrees of freedom (wet and dry, including interior points), and  $f$  is the number of fluid degrees of freedom (DOF) on the fluid-structure interface. That is,  $f$  is equal to the number of wet points.

However, in terms of the wet DOF of the problem, the applied forces and the resulting velocities are related by

$$(z_s + Z_f) v = F^{(n)} \quad (19)$$

where  $v$  = complex amplitude of the velocity vector for the wet DOF (the surface normals)

$F^{(n)}$  = complex amplitude of the force vector applied to the wet DOF

$z_s$  = impedance matrix for the structure in terms of the wet DOF

$Z_f$  = impedance matrix for the exterior fluid

The structural impedance matrix  $Z_s$  and applied load vector  $F$  expressed in terms of all structural DOF can be related to the smaller matrices  $z_s$  and  $F^{(n)}$  using

the transformation matrix G defined by the equation

$$F = G F^{(n)} \quad (20)$$

where F is a vector of dimension s (the total number of structural DOF),  $F^{(n)}$  is a vector of dimension f (the number of fluid (wet) DOF on the surface), and G is the s x f matrix of direction cosines which converts  $F^{(n)}$  to F. Thus,

$$z_s^{-1} = G^T Z_s^{-1} G \quad (21)$$

$$z_s^{-1} F^{(n)} = G^T Z_s^{-1} F \quad (22)$$

where the latter equation indicates the transformation of the velocity vector. Algebraic manipulation of the preceding four equations yields [6,7]

$$H p = Q \quad (23)$$

where

$$H = E + C G^T Z_s^{-1} G A \quad (24)$$

$$Q = C G^T Z_s^{-1} F \quad (25)$$

Matrices E, C, and A have dimension f x f,  $Z_s$  is s x s, G is s x f, and F is s x r, where s is the number of structural DOF, f is the number of fluid DOF (on the wet surface), and r is the number of load cases. Since H and Q depend on geometry, material properties, and frequency, Equation (23) may be solved to yield the surface pressures p. Surface normal velocities 'v' may then be recovered using

$$v = G^T Z_s^{-1} F - G^T Z_s^{-1} G A p \quad (26)$$

To summarize, the NASHUA solution procedure uses NASTRAN to generate K, M, B, and F and to generate sufficient geometry information so that E, C, G, and A can be computed by a separate program (SURF). Then, given all matrices on the right-hand sides of Equations (24) and (25), a NASTRAN DMAP analysis is used to compute H and Q. Equation (23) is then solved for the pressures 'p' using a new block solver (OCSOLVE) written especially for this problem. Next, NASTRAN DMAP is used to recover the surface velocities 'v' according to Equation (26). This completes the surface solution.

### The Far-Field Solution

Given the solution for the pressures and velocities on the surface, the exterior Helmholtz integral equation, Equation (4), can be integrated to obtain the radiated pressure at any desired location  $\underline{x}'$  in the field. We first substitute Equations (6) and (7) into Equation (4) to obtain a form suitable for numerical integration:

$$p(\underline{x}') = \int_S [i\omega\rho v(\underline{x}) + (ik + 1/r)p(\underline{x}) \cos \beta] (e^{-ikr}/4\pi r) dS \quad (27)$$

where all symbols have the same definitions as were used previously, and  $\underline{x}'$  is in the exterior field. Thus, given the pressure  $p$  and normal velocity  $v$  on the surface  $S$ , the pressure at  $\underline{x}'$  can be determined by numerical quadrature using Equation (27).

In applications, however, the field pressures generally of interest are in the far-field, so we develop an asymptotic form of Equation (27) for use instead of Equation (27). In the far-field,  $x' \rightarrow \infty$  implies

$$ik + 1/r \rightarrow ik \quad (28)$$

$$\cos \beta \rightarrow \underline{n} \cdot \underline{x}' / x' \quad (29)$$

and, from the application of the law of cosines,

$$r \rightarrow x' - x \cos \alpha \quad (30)$$

where  $\alpha$  is defined in Figure 1. Hence, in the far-field [6],

$$p(\underline{x}') = (ike^{-ikx'} / 4\pi x') \int_S [\rho cv(\underline{x}) + p(\underline{x}) \cos \beta] e^{ikx \cos \alpha} dS \quad (31)$$

where the asymptotic form, Equation (29), is used for  $\cos \beta$ . We note that, since Equation (31) is a far-field formula, the pressure varies inversely with distance  $x'$  everywhere so that any range  $x'$  may be used in its evaluation, e.g., 36 inches (one yard). Numerically, the integral in Equation (31) is evaluated as

$$p(x') = (ike^{-ikx'} / 4\pi x') \sum_j (\rho cv_j + p_j \cos \beta_{ij}) e^{ikx \cos \alpha} A_j \quad (32)$$

#### Other Output Quantities

Given both the surface and far-field solutions, a variety of other quantities of interest in applications can be computed. The average and root-mean-square normal velocities on the surface are defined as

$$v_{avg} = \int_S v dS / A \approx \sum_i v_i A_i / A \quad (33)$$

$$v_{rms} = (\int_S |v|^2 dS / A)^{1/2} \approx (\sum_i |v_i|^2 A_i / A)^{1/2} \quad (34)$$

where  $A$  is the total area of the radiating surface. The volume velocity, a measure of source strength, is  $Av_{avg}$ . Average and rms surface pressures can also be computed using Equations similar to (33) and (34) if ' $v$ ' is replaced by ' $p$ '.

The acoustic intensity at a point on the surface is the product of the pressure there with the component of normal velocity which is in phase with the pressure:

$$I = \text{Re}(pv^*) \quad (35)$$

where the asterisk denotes the complex conjugate. (There is no factor 1/2 in Equation (35) if we assume that pressures and velocities are already "effective" values rather than amplitudes.)

The power radiated can be obtained by integrating the acoustic intensity over the surface

$$W_{\text{rad}} = \int_S \text{Re}(pv^*) dS \approx \sum_i \text{Re}(p_i v_i^*) A_i \quad (36)$$

Since for low frequencies,  $p$  and  $v$  are nearly orthogonal (i.e., the fluid behaves like an added mass), this integral can be sensitive to small errors in  $p$  and  $v$  on the surface. To circumvent this problem, the radiated power is also computed by integrating the acoustic intensity over the far-field sphere, where  $p = \rho cv$ :

$$W_{\text{rad}} = \int_{S_0} (|p|^2/\rho c) dS_0 \approx \sum_i |p_i|^2 A_{oi}/\rho c \quad (37)$$

where  $S_0$  is the surface of the far-field sphere, and the numerical approximation is summed over all far-field points where pressure is evaluated. For a non-dissipative medium, the last two equations are theoretically equivalent. Numerically, the second form, Equation (37), is better behaved, but it has the slight disadvantage of requiring the computation of the far-field solution at a large enough number of points so that the integration can be accurately performed.

Given the power radiated and the rms surface velocity, the radiation efficiency  $\sigma$  can be computed:

$$\sigma = W_{\text{rad}}/(\rho c A v_{\text{rms}}^2) \quad (38)$$

where  $v_{\text{rms}}^2$  is the mean-square velocity on the surface, and  $A$  is the area of the surface [15].

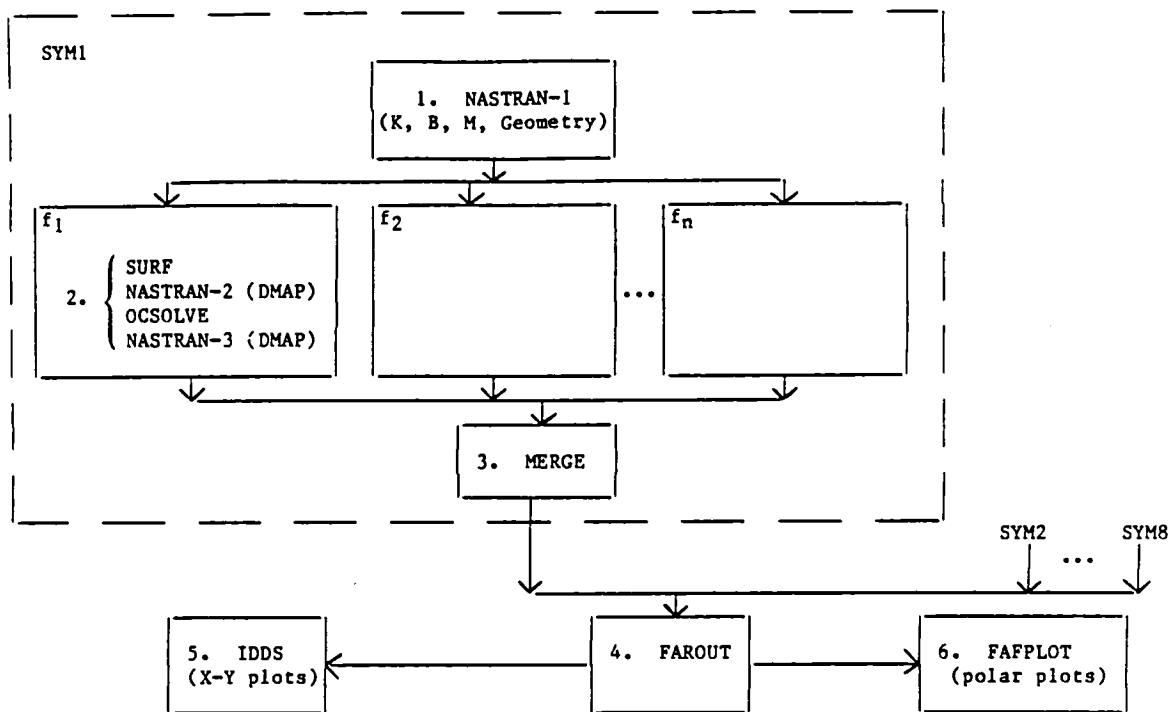
#### OVERVIEW OF NASHUA SOLUTION PROCEDURE

The overall organization and setup of the solution procedure is summarized in Figure 2. NASTRAN appears three times in the procedure; to distinguish one NASTRAN execution from another, the integers 1, 2, or 3 are appended to "NASTRAN" in the figure.

A separate NASTRAN model is prepared and run (Step 1 in Figure 2) for each unique set of symmetry constraints. Since up to three planes of reflective symmetry are allowed, there would be one, two, four, or eight such runs. Step 1 generates files containing geometry information and the structure's stiffness (K), mass (M), and damping (B) matrices.

For each symmetry case and drive frequency, the Step 2 sequence is run in a single job. The SURF program reads the geometry file generated by NASTRAN in Step 1 and, using the Helmholtz surface integral equation, generates the fluid matrices E and C for the exterior fluid, the area matrix A, the structure-fluid transformation matrix G, and a condensed geometry file to be used later by FAROUT (Step 4) for the field calculation. SURF is followed by a NASTRAN DMAP job which takes the matrices K, M, B, and F from Step 1 and the matrices E, C, A, and G from SURF and calculates H and Q according to Equations (24) and (25). Equation (23) is then solved for the surface pressure vector 'p' by program OCSOLVE. OCSOLVE is a general block solver for full, complex, nonsymmetric systems of linear, algebraic equations. The program was designed to be particularly effective on such systems and executes about 20 times faster than NASTRAN's equation solver,





NOTE: Each solid block is a separate job submission.

Figure 2 - Summary of NASHUA Solution Procedure

which was not designed for efficient solution of such systems of equations. NASTRAN is then re-entered in Step 2 with 'p' so that the outward normal surface velocity vector 'v' can be recovered using DMAP operations according to Equation (26). A file containing the surface pressures and velocities for each unique symmetry case and frequency is saved at the conclusion of Step 2.

After all frequencies have been run for a given symmetry case, the surface pressure and velocity results are reformatted and merged into a single file using program MERGE (Step 3). This program is run separately for each symmetry case. Recall that there are one, two, four, or eight possible symmetry cases.

Steps 1 to 3 are repeated for each symmetry case. After all symmetry cases are completed (with Step 3 completed for each), program FAROUT (Step 4) is run to combine the symmetry cases and to integrate over the surface. FAROUT uses as input the geometry file generated by SURF (Step 2) and the surface solutions from the one, two, four, or eight files generated by MERGE (Step 3). The far-field pressure solution is obtained by integrating the surface pressures and velocities using the far-field form of the exterior Helmholtz integral equation, Equation (31). Output from FAROUT consists of both tables and files suitable for plotting by IDDS (Step 5) and FAFPLOT (Step 6).

IDDS (Step 5) is a general purpose interactive X-Y plotting program which is used here for plotting surface velocities and impedances versus frequency [16]. FAFPLOT (Step 6) is an interactive graphics program for making polar plots of the

far-field sound pressure levels in each of the three principal coordinate planes [17].

Complete details on the requirements and deck setups for the entire solution procedure are given in the NASHUA user's guide [11].

#### FREQUENCY LIMITATIONS

It is known that the fluid matrices E and C in the surface Helmholtz integral equation formulation are singular at the frequencies of the resonances of the corresponding interior acoustic cavity with Dirichlet (zero pressure) boundary conditions [5]. Although the NASHUA formulation described in the previous section was designed to avoid having to invert either E or C in Equations (23) to (25), the coefficient matrix H is also poorly conditioned at these frequencies (referred to as the "critical" or "forbidden" frequencies of the problem). Therefore, to be safe, the user should avoid excitation frequencies which exceed the lowest critical frequency for the geometry in question.

For spheres, for example, the lowest critical frequency occurs at  $ka = \pi$ . For long cylinders with flat ends, the lowest critical frequency occurs at  $ka \approx 2.4$ , where k is the acoustic wave number, and 'a' is the radius of the sphere or cylinder. For short cylinders with flat ends, the lowest critical frequency is slightly higher than for long cylinders.

#### RESTRICTIONS ON MODEL

Although the NASHUA solution procedure was designed to be general enough so that arbitrary three-dimensional structures could be analyzed, a few restrictions remain. In our view, however, none is a burden, since a NASTRAN deck for a dry structure modeled with low-order finite elements can be adapted for use with NASHUA in a few hours. The following general restrictions apply:

1. All translational DOF for wet points must be in NASTRAN's "analysis set" (a-set), since (a) all symmetry cases must have the same wet DOF, and (b) the fluid matrices E and C involve all wet points. This restriction also affects constraints. Thus, constraints on translational DOF of wet points may not be imposed with single point constraint (SPC) cards, but must instead be imposed using large springs connected between ground and the DOF to be constrained. Generally, this restriction affects only those DOF which are constrained due to symmetry conditions.

2. The wet face of each finite element in contact with the exterior fluid must be defined by either three or four grid points, since the numerical discretization of the Helmholtz surface integral equation assumes the use of low order elements. In particular, NASTRAN elements with midside nodes (e.g., TRIM6, IS2D8, or IHEX2) may not be in contact with the exterior fluid.

3. Symmetry planes must be coordinate planes of the basic Cartesian coordinate system.

4. No scalar points or extra points are allowed, since program SURF assumes that each point is a grid point.

5. For cylindrical shells, the axis of the cylinder should coincide with one of the three basic Cartesian axes; for spherical shells, the center of the sphere should coincide with the basic origin. These restrictions facilitate the treatment of symmetry planes and the calculation of curvatures in program SURF.

6. At least one degree of freedom in the model should be constrained with an SPC, MPC, or OMIT so that the NASTRAN data block PL is generated.

7. Thin structures with fluid on both sides should be avoided, since the formulations for the fluid matrices are singular if two wet points are coincident. A precise restriction is not known.

#### TIME ESTIMATION

Most of the computer time required to execute the entire NASHUA procedure is associated with the back solve operation (FBS) in Step 2, Equation (24), in which the matrix  $Z_s^{-1}GA$  is computed given the triangular factors of  $Z_s$  and the matrix  $GA$ .  $Z_s$  is a complex, symmetric, banded matrix of dimension  $s \times s$ , where  $s$  is the number of structural DOF in the problem, and  $GA$  is a real, sparsely-populated, rectangular matrix of dimension  $s \times f$ , where  $f$  is the number of fluid DOF (the number of wet points on the surface). This FBS time is proportional to  $f$  and typically accounts for about two-thirds of the total time to make a single pass through the NASHUA procedure.

For example, consider a problem with the following characteristics:

$$\begin{aligned} s &= 2973 \quad (\text{number of structural DOF}) \\ f &= 496 \quad (\text{number of fluid DOF}) \\ W_{\text{avg}} &= 129 \quad (\text{average wavefront of stiffness matrix}) \end{aligned}$$

On the CDC Cyber 176 computer at DTNSRDC, the computer time ("wall-clock" time) required to solve this problem in a dedicated computer environment for a single symmetry case and one drive frequency was about 30 minutes, of which 19 minutes were spent in the FBS operation.

#### EXAMPLE 1: UNIFORMLY-DRIVEN SPHERICAL SHELL

We first demonstrate NASHUA's ability to solve radiation problems by solving the problem of the uniformly-driven submerged spherical shell, a problem with a closed-form solution. In this problem, a thin-walled spherical shell is submerged in a liquid and driven internally with a spherically-symmetric time-harmonic pressure load. Since the solution is also spherically-symmetric, the field solution depends only on radial distance from the origin.

#### Analytic Solution

The shell stiffness (the total static force required to increase the radius a unit amount) is

$$k_s = 8\pi Eh/(1-\nu) \quad (39)$$

where  $E$  and  $\nu$  are the Young's modulus and Poisson's ratio for the shell material, and  $h$  is the thickness of the shell. The shell mass is

$$m_s = 4\pi a^2 h \rho_s \quad (40)$$

where 'a' is the mean shell radius, and  $\rho_s$  is the density of the shell material. Hence, for a uniform time-harmonic pressure drive, the structural impedance is

$$Z_s = (\omega^2 m_s - k_s) i / \omega \quad (41)$$

where  $\omega$  is the circular frequency of the excitation.

For the surrounding fluid, the ratio of surface pressure to surface velocity is [5]

$$p/v = i\omega\rho a / (1 + ika) \quad (42)$$

where  $\rho$  is the density of the fluid and  $k = \omega/c$ . Hence, the fluid impedance (ratio of total force to velocity) is

$$Z_f = i\omega\rho 4\pi a^3 / (1 + ika) \quad (43)$$

For the harmonically-driven submerged shell, the surface velocity is therefore

$$v = 4\pi a^2 p_o / (Z_s + Z_f) \quad (44)$$

where  $p_o$  is the amplitude of the internal pressure drive. The surface pressure can be recovered from Equation (42). The fluid pressure in the exterior field decays inversely with distance [18]; hence

$$p_r = p(a/r) e^{-ik(r-a)} \quad (45)$$

where  $p_r$  is the pressure at distance  $r$  from the origin, and  $p$  is the pressure on the surface. Note that if the expression for surface velocity  $v$  obtained from Equation (42) is substituted into the far-field radiated pressure formula, Equation (31), Equation (45) is obtained.

The radiation efficiency for this problem is obtained by substituting the surface solution, Equation (42), into Equations (36) and (38):

$$\sigma = (ka)^2 / (1 + (ka)^2) \quad (46)$$

#### NASHUA Solution

We solve with NASHUA the problem with the following characteristics [19]:

$a = 5$ m	(shell radius)
$h = 0.15$ m	(shell thickness)
$E = 2.07 \times 10^{11}$ Pa	(Young's modulus)
$\nu = 0.3$	(Poisson's ratio)
$\rho_s = 7669$ kg/m <sup>3</sup>	(shell density)
$\rho = 1000$ kg/m <sup>3</sup>	(fluid density)
$c = 1524$ m/s	(fluid speed of sound)
$p_o = 1$ Pa	(internal pressure)

One octant of the shell was modeled with NASTRAN's CTRIA2 membrane/bending elements as shown in Figure 3. With 20 elements along each edge of the domain, the model has 231 wet points and 1263 structural DOF. Three planes of symmetry were imposed.

The NASHUA model was run for 15 drive frequencies in the nondimensional frequency range  $ka = 0.5$  to  $ka = 8.0$ , where 'a' is the shell radius. Table 1 shows a comparison between the NASHUA calculations and the closed-form solution for surface pressures, surface velocities, and far-field radiated pressures. Clearly, the NASHUA calculations agree very closely with the closed-form solution for all  $ka$ 's except those near  $ka = \pi$  and  $ka = 8.18$ , where the Helmholtz integral equation is singular [19], as discussed in a previous section.

#### EXAMPLE 2: SECTOR-DRIVEN SPHERICAL SHELL

The uniformly-driven spherical shell problem described in the preceding section is necessary but probably not sufficient to validate NASHUA. A more challenging problem, both analytically and numerically, is the spherical shell with a uniform pressure drive over a sector, as shown in Figure 4. (Here we use the term "analytic" to refer to a series solution which converges to the exact solution.) The particular problem solved has the internal pressure load applied over the polar angle  $\gamma = 36$  degrees.

This problem was solved with the same finite element model used in Example 1. Thus, with two load cases (subcases), both problems can be solved together. However, with a one-octant model of the sphere (Figure 3), the NASHUA solution of this problem requires running both symmetric and anti-symmetric parts of the

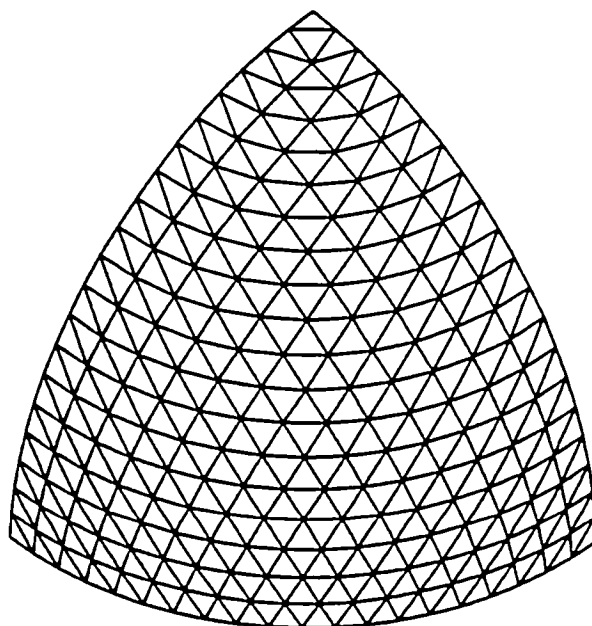


Figure 3 - Finite Element Model of One Octant of Spherical Shell

Table 1 - Comparison of NASHUA Solution with Closed-Form Solution for Uniformly-Driven Spherical Shell

ka	Average Surface Pressure			Average Surface Velocity			Far-Field Pressure		
	NASHUA	Exact	% Error	NASHUA	Exact	% Error	NASHUA*	Exact	% Error
	(x10 <sup>-1</sup> )	(x10 <sup>-1</sup> )		(x10 <sup>-7</sup> )	(x10 <sup>-7</sup> )		(x10 <sup>-2</sup> )	(x10 <sup>-2</sup> )	
0.5	0.302	0.303	0.3	0.445	0.444	0.2	0.151	0.151	0.0
1.0	1.02	1.02	0.0	0.948	0.947	0.1	0.508	0.510	0.4
1.5	1.91	1.92	0.5	1.51	1.51	0.0	0.944	0.958	1.5
2.0	2.92	2.92	0.0	2.14	2.14	0.0	1.48	1.46	1.4
2.5	4.04	4.03	0.2	2.84	2.85	0.4	2.04	2.02	1.0
2.8	4.80	4.76	0.8	3.28	3.32	1.2	2.42	2.38	1.7
3.0	5.41	5.28	2.5	3.54	3.65	3.0	2.73	2.64	3.4
3.1	6.10	5.54	10.1	3.41	3.82	10.7	3.07	2.77	10.8
3.14	10.1	5.65	78.8	0.231	3.89	94.1	5.05	2.82	79.1
3.2	5.35	5.81	7.9	4.35	4.00	8.8	2.69	2.91	7.6
3.3	5.89	6.09	3.3	4.32	4.17	3.6	2.96	3.04	2.6
3.5	6.53	6.64	1.7	4.61	4.53	1.8	3.29	3.32	0.9
4.0	7.97	8.04	0.9	5.50	5.44	1.1	4.01	4.02	0.2
5.0	9.97	10.0	0.3	6.75	6.70	0.7	5.10	5.01	1.8
8.0	7.02	7.04	0.3	4.82	4.65	3.7	3.73	3.52	6.0

\* worst case

- Notes:
1. The average surface velocity is defined in Equation (33); the average surface pressure is similarly defined.
  2. The "% Error" is defined as  $100 * |NASHUA - Exact| / Exact$
  3. SI units are used (Pa for pressure and m/s for velocity). Far-field pressures are calculated at a range of 100m.
  4. The NASHUA far-field pressure used is the one on the far-field sphere which deviates the most in absolute value from the exact result.
  5. The critical frequencies which affect these calculations are located at  $ka = \pi$  and  $ka = 8.18$ .

problem, thus providing a good check on NASHUA's ability to combine symmetry cases.

The benchmark solution to which the NASHUA results are compared is a series solution which we developed based on equations in the Junger and Feit book [20]. The results of this comparison are shown in Table 2 for four different non-dimensional drive frequencies  $ka$ , where 'a' is the radius of the sphere. None of the drive frequencies is near a critical frequency. For each drive frequency  $ka$ , the normalized far-field pressure  $|p_{r,r}/p_{0a}|$  is listed for each colatitude angle  $\theta$ ,

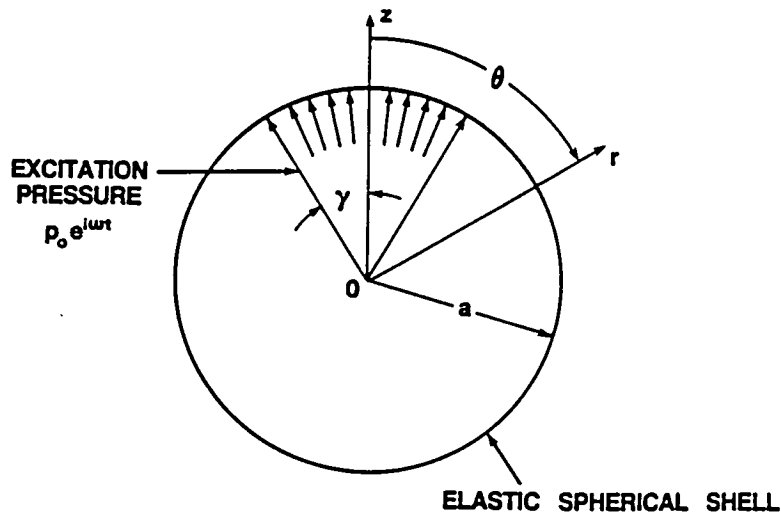


Figure 4 - Submerged Elastic Spherical Shell Driven over Sector

where  $p_r$  is the far-field pressure at distance  $r$  from the origin, and  $p_0$  is the internally-applied pressure. Clearly, the NASHUA solution again agrees very well with the exact solution.

#### DISCUSSION

A very general capability has been described for predicting the acoustic sound pressure field radiated by arbitrary three-dimensional elastic structures subjected to time-harmonic loads. Sufficient automation is provided so that, for many structures of practical interest, an existing NASTRAN structural model can be adapted for NASHUA acoustic analysis within a few hours.

One of the major benefits of having NASHUA linked with NASTRAN is the ability to integrate the acoustic analysis of a structure with other dynamic analyses. Thus the same finite element model can be used for modal analysis, frequency response analysis, linear shock analysis, and underwater acoustic analysis. In addition, many of the pre- and postprocessors developed for use with NASTRAN become available for NASHUA as well.

There are two areas in which improvements to NASHUA would be desirable. The first is to remove the frequency limitation caused by the presence of the critical frequencies inherent in the Helmholtz integral equation formulation. As a result, cylindrical shells, for example, can be safely analyzed by NASHUA only for  $ka < 2.4$ , where 'a' is the radius. Since for some problems, it would be of interest to treat higher frequencies, the limitation should be removed. A conversion to a different formulation (e.g., Burton and Miller [8] or Mathews [10]) is being considered.

The second area in which NASHUA could be improved would be to extend the program's capabilities to include acoustic scattering as well as radiation. Generally, this improvement requires replacing the mechanical drive force with an incident loading, a relatively modest change [2].

Table 2 - Comparison of NASHUA Solution with Converged Series Solution for Sector-Driven Spherical Shell

ka	Colatitude $\theta$ (degrees)	Normalized Far-Field Pressure, $p_{rr}/p_{0a}$		
		NASHUA	Exact	% Error
0.5	0	0.0514	0.0514	0.0
	30	0.0445	0.0445	0.0
	60	0.0257	0.0258	0.4
	90	0.0035	0.0035	0.0
	120	0.0258	0.0259	0.4
	150	0.0446	0.0446	0.0
	180	0.0515	0.0515	0.0
1.0	0	0.0887	0.0889	0.2
	30	0.0744	0.0745	0.1
	60	0.0434	0.0434	0.0
	90	0.0235	0.0237	0.8
	120	0.0448	0.0448	0.0
	150	0.0784	0.0786	0.3
	180	0.0939	0.0942	0.3
2.0	0	1.183	1.163	1.7
	30	0.278	0.276	0.7
	60	0.667	0.666	0.2
	90	0.131	0.128	2.3
	120	0.721	0.716	0.7
	150	0.757	0.695	8.9
	180	1.977	1.860	6.3
5.0	0	0.510	0.512	0.4
	30	0.292	0.292	0.0
	60	0.020	0.017	17.6
	90	0.100	0.097	3.1
	120	0.161	0.160	0.6
	150	0.169	0.163	3.7
	180	0.177	0.170	4.1

#### REFERENCES

1. Everstine, G.C., "A Symmetric Potential Formulation for Fluid-Structure Interaction," J. Sound and Vibration, vol. 79, no. 1, pp. 157-160 (1981).
2. Everstine, G.C., "Structural-Acoustic Finite Element Analysis, with Application to Scattering," Proc. 6th Invitational Symposium on the Unification of Finite Elements, Finite Differences, and Calculus of Variations, ed. by H. Kardestuncer, Univ. of Connecticut, pp. 101-122 (1982).



3. Kalinowski, A.J., and C.W. Nebelung, "Media-Structure Interaction Computations Employing Frequency-Dependent Mesh Sizes with the Finite Element Method," The Shock and Vibration Bulletin, vol. 51, part 1, pp. 173-193 (1981).
4. Chen, L.H., and D.G. Schweikert, "Sound Radiation from an Arbitrary Body," J. Acoust. Soc. Amer., vol. 35, no. 10, pp. 1626-1632 (1963).
5. Schenck, H.A., "Improved Integral Formulation for Acoustic Radiation Problems," J. Acoust. Soc. Amer., vol. 44, no. 1, pp. 41-58 (1968).
6. Henderson, F.M., "A Structure-Fluid Interaction Capability for the NASA Structural Analysis (NASTRAN) Computer Program," Report 3962, David Taylor Naval Ship R&D Center, Bethesda, Maryland (1972).
7. Wilton, D.T., "Acoustic Radiation and Scattering From Elastic Structures," Int. J. Num. Meth. in Engrg., vol. 13, pp. 123-138 (1978).
8. Burton, A.J., and G.F. Miller, "The Application of Integral Equation Methods to the Numerical Solution of Some Exterior Boundary-Value Problems," Proc. Roy. Soc. Lond. A, vol. 323, pp. 201-210 (1971).
9. Baron, M.L., and J.M. McCormick, "Sound Radiation from Submerged Cylindrical Shells of Finite Length," ASME Trans. Ser. B, vol. 87, pp. 393-405 (1965).
10. Mathews, I.C., "A Symmetric Boundary Integral-Finite Element Approach for 3-D Fluid Structure Interaction," in Advances in Fluid-Structure Interaction - 1984, PVP-Vol. 78 and AMD-Vol. 64, ed. by G.C. Everstine and M.K. Au-Yang, American Society of Mechanical Engineers, New York, pp. 39-48 (1984).
11. Everstine, G.C., "User's Guide to the Coupled NASTRAN/Helmholtz Equation Acoustic Radiation Capability (NASHUA)," Report CMLD-86/03, David Taylor Naval Ship R&D Center, Bethesda, Maryland (1986).
12. Lamb, H., Hydrodynamics, sixth ed., Dover Publications, New York (1945).
13. Vandergraft, J.S., Introduction to Numerical Computations, second ed., Academic Press, New York (1983).
14. Chertock, G., "Integral Equation Methods in Sound Radiation and Scattering from Arbitrary Surfaces," Report 3538, David Taylor Naval Ship R&D Center, Bethesda, Maryland (1971).
15. Ghering, W.C., Reference Data for Acoustic Noise Control, Ann Arbor Science Publishers, Inc., Ann Arbor, Michigan (1978).
16. Marquardt, M.B., "DIGIT: The Curve Digitizing Subsystem of the Interactive Data Display System," Report DTNSRDC-80/038, David Taylor Naval Ship R&D Center, Bethesda, Maryland (1980).
17. Lipman, R.R., "Calculating Far-Field Radiated Sound Pressure Levels from NASTRAN Output," 14th NASTRAN Users' Colloquium, National Aeronautics and Space Administration, Washington, DC (1986) (this volume).

18. Kinsler, L.E., A.R. Frey, A.B. Coppens, and J.V. Sanders, Fundamentals of Acoustics, third ed., John Wiley and Sons, New York (1982).

19. Huang, H., and Y.F. Wang, "Asymptotic Fluid-Structure Interaction Theories for Acoustic Radiation Prediction," J. Acoust. Soc. Amer., vol. 77, no. 4, pp. 1389-1394 (1985).

20. Junger, M.C., and D. Feit, Sound, Structures, and Their Interaction, The MIT Press, Cambridge, Massachusetts (1972).